Molecular Therapy
Original Article

Combined Ectopic Expression of Homologous Recombination Factors Promotes Embryonic Stem Cell Differentiation

Eui-Hwan Choi,[1] Seobin Yoon,[1] and Keun P. Kim[1]

[1]Department of Life Sciences, Chung-Ang University, Seoul 156-756, South Korea

Homologous recombination (HR), which ensures accurate DNA replication and strand-break repair, is necessary to preserve embryonic stem cell (ESC) self-renewal. However, little is known about how HR factors modulate ESC differentiation and replication stress-associated DNA breaks caused by unique cell-cycle progression. Here, we report that ESCs utilize Rad51-dependent HR to enhance viability and induce rapid proliferation through a replication-coupled pathway. In addition, ESC differentiation was shown to be enhanced by ectopic expression of a subset of recombinases. Abundant expression of HR proteins throughout the ESC cycle, but not during differentiation, facilitated immediate HR-mediated repair of single-stranded DNA (ssDNA) gaps incurred during S-phase, via a mechanism that does not perturb cellular progression. Intriguingly, combined ectopic expression of two recombinases, Rad51 and Rad52, resulted in efficient ESC differentiation and diminished cell death, indicating that HR factors promote cellular differentiation by repairing global DNA breaks induced by chromatin remodeling signals. Collectively, these findings provide insight into the role of key HR factors in rapid DNA break repair following chromosome duplication during self-renewal and differentiation of ESCs.

INTRODUCTION

ESCs can differentiate into diverse cell types, through the formation of all three germ layers (mesoderm, endoderm, and ectoderm), following proper signaling.[1,2] To maintain characteristics of pluripotency and self-renewal, genomic stability must be maintained through faithful DNA replication. Accordingly, spontaneous mutations associated with discontinued progression of the replication fork, uncontrolled assembly of the replication machinery, and spatiotemporal dysregulation of replication factors must be avoided.[3–5] If DNA damage is not properly repaired, mutations can accumulate as cells grow and divide, ultimately modifying the genes that are inherited by daughter cells. Such mutations might affect the fundamental characteristics of cells, leading to unprogrammed differentiation and abnormal growth. Therefore, ESCs have acquired error-free DNA repair abilities and effective mechanisms to avoid mutations and phase arrest throughout the cell cycle.[3,4,6]

DNA repair mediated by homologous recombination (HR) is essential for the preservation of genomic integrity, and the regulatory mechanisms of HR have been characterized in diverse organisms, including plant, animal, and yeast.[7–10] HR is a major DNA metabolic pathway that facilitates high-fidelity repair of DNA gaps, interstrand crosslinks (ICLs), and double-strand breaks (DSBs).[7,11] HR is crucial for promoting mitosis by repairing broken replication forks that mainly occur in late S- and G2-phases, and during the genetic exchange between homologous chromosomes that creates non-identical haploid gametes during meiotic cell division.[7,12–14] Moreover, several human cancers associated with genomic instability can be caused by defects in HR or associated processes.[15,16] Mammalian Rad51 is homologous to bacterial RecA and yeast Rad51, which are also essential for DNA replication, DNA repair, and genetic recombination.[17,18] Accessory factors for Rad51, including BRCA1/2, PALB2, Rad51AP1, Rad52, and Rad54, enhance its strand-exchange activity.[7,19–21] These accessory proteins facilitate the timely formation of Rad51-single-stranded DNA (ssDNA) filaments to promote homologous pairing. During homologous pairing, Rad51 and its accessory factors search for DNA homologs and perform DNA-strand exchange, generating a D-loop that is a pre-form of the single-strand invasion that primes DNA synthesis.[7] Loss of these controls due to functional defects in HR proteins is a key event leading to cell death, genomic instability, and tumorigenesis.

The chromatin of ESCs undergoes dramatic reorganization during the differentiation process,[22] thereby inducing various types of DNA damage. ESCs exhibit a robust HR-mediated DNA damage response that ensures preservation of genomic integrity throughout the cell cycle.[23–25] Previously, we discovered that Rad51 disruption causes incomplete chromosome separation and reduces the efficiency of ESC proliferation.[26] However, it is unclear how ESCs regulate HR machinery to cope with the DNA breaks caused by global chromatin remodeling during differentiation and replication-associated stress following the S-phase during normal growth. It is also unknown why HR is actively involved in ESC-cycle progression.

Received 6 January 2018; accepted 5 February 2018;
https://doi.org/10.1016/j.ymthe.2018.02.003.

Correspondence: Keun P. Kim, Department of Life Sciences, Chung-Ang University, Seoul 156-756, South Korea.
E-mail: kpkim@cau.ac.kr

In this study, we provide concrete and comprehensive evidence that ESCs constitutively express key HR proteins throughout the cell cycle, but not during differentiation, which immediately localize to chromosome breaks during the S-phase. Remarkably, ectopic expression of the strand-exchange factors, Rad51 and Rad52, was found to effectively promote ESC differentiation and limit differentiation-induced cell death. Moreover, we showed that ESCs depleted of Rad51 exhibited larger ssDNA gaps, which did not prevent S/G2-phase progression. Subsequent high-throughput RNA sequencing (RNA-seq) experiments revealed dynamic changes in the expression of regulatory genes involved in programmed cell death, cell proliferation, and cell-cycle progression in response to *RAD51* knockdown. Collectively, these data suggest that ESCs exhibit increased expression of HR proteins, which allows cells to rapidly overcome the accumulation of ssDNA gaps and DNA breaks, thereby contributing to efficient cell proliferation and differentiation.

RESULTS

HR Factors Are Abundantly Expressed in ESCs throughout the Cell Cycle, but Not during Differentiation

Rad51 and other HR-related accessory factors are essential for DNA break-induced damage repair and participate in tightly controlled recombination mechanisms.[7] To understand the means through which mouse ESCs (mESCs) maintain their potential for self-renewal, we examined the cell-cycle profiles and expression pattern of HR factors involved in Rad51-mediated strand displacement and DNA-break resection in mESCs, mouse embryonic fibroblasts (MEFs), and human embryonic stem cells (hESCs) by fluorescence-activated cell sorting (FACS) analysis and western blotting, respectively. Notably, mESCs and hESCs displayed a marked increase in actively replicating cells as compared with MEFs (Figure S1A). Moreover, the expression levels of Rad51, Rad54, and Exo1 were higher in ESCs than in MEFs (Figure S1B), indicating that these factors are related to the enhanced HR activity of ESCs (Figure 1B). Thus, HR-mediated genomic stability might be important for ESC pluripotency and self-renewal.

Because mESCs exhibit constitutive HR protein expression (Figure S1C), we wondered whether this expression is maintained during cellular differentiation. To examine the expression kinetics of HR proteins in mESCs during differentiation, we added 0.2 μM retinoic acid (RA) to induce mESC differentiation (Figure 1A). Interestingly, the levels of the HR proteins Rad51, Rad54, and Exo1 gradually decreased with RA treatment in a time-dependent manner (Figures 1B and S1D), and this sensitized cells to DNA damage-induced cell death (Figure S2).

Global Chromatin Expansion in mESCs

Chromosome structure undergoes cyclic global fluctuations between compaction and expansion states, which differ between mESCs and differentiated cells.[27,28] Changes in chromosome condensation could be associated with the expression of diverse genes. To understand chromatin morphology in mESCs and differentiated cells, we analyzed chromosome volume and length from prophase to metaphase using histone H2B-GFP and by fluorescence microscopy (Figures 1C–1F). The length analysis indicated that chromosome length is apparently shorter in differentiated cells than in mESCs during prophase; in addition, chromosome volume was reduced significantly in differentiated cells from mid-prophase to metaphase. Thus, chromosome expansion in mESCs results from an increase in chromosome length with changes in chromatin condensation, whereas compaction in differentiated cells results from a dramatic decrease in length.

HR Factors Assemble at ssDNA Gaps during S-Phase in mESCs

We previously reported that the recruitment of Rad51 to chromatin occurs in the absence of DNA damage under normal ESC-cycle conditions,[26] and here that mESCs abundantly express diverse HR factors throughout the entire cell cycle (Figure S1). To identify the cell-cycle phases that require HR factors in mESCs, we examined the co-localization of HR proteins with γH2AX in synchronized mESCs (Figures 2A and S3A). Consistent with our previous findings, approximately 85% of cells synchronized to the G1/S-phase after the double-thymidine block, whereas 43% of unsynchronized cells were in the S-phase (Figures S3B and S3C). To quantitatively analyze co-localization, we grouped cells positive for Exo1, Rad51, Rad54, and proliferating cell nuclear antigen (PCNA) foci into four categories as follows: class I, no foci; class II, 1–5 foci; class III, 6–25 foci; class IV, $\geq$26 foci (Figure S4). Interestingly, more than 82% of mESCs in S-phase contained greater than 5 foci, and 35% of mESCs in G2/M-phase contained greater than 5 foci (Figures 2A, 2B, and S4; also see Figure S5). Moreover, Rad51, Rad54, Exo1, and PCNA foci formation was highly correlated with the stage of cell cycle, specifically in S-phase (Figure 2C). Based on these data, we surmised that the high number of ssDNA gaps/DNA breaks observed in mESCs might be caused by prolonged DNA replication, perhaps as a result of inefficient completion of post-replicative steps. We therefore reasoned that the abundant HR machinery in mESCs can be quickly and effectively recruited to replication-associated ssDNA gaps/DNA breaks originating from prolonged S-phase.

mESCs Upregulate a Broad Range of HR Factors Relative to Expression in Differentiated Cells

HR factors are required for proper DNA replication or the recovery of replication problems encountered by replisome components. Thus, the replication-coupled HR pathway is necessary to ensure that rapid replication resumes following replication fork stalling or ssDNA gaps. mESCs constitutively expressed substantial levels of HR factors, regardless of the cell-cycle phase, and HR proteins are actively assembled on the chromatin during S-phase, but whether the expression patterns of multiple HR proteins and auxiliary factors are critically relevant to the cell cycle had not been determined. To characterize HR factor expression patterns during cellular progression, we performed global transcript analysis by RNA-seq at specific cell-cycle phases using MEFs and mESCs synchronized at the S-phase (Figures 2D–2F; Table S1). For this, genes involved in the regulation of HR were classified into three groups: DSB resection, ssDNA annealing, and synapse (Figure 2E). Our results demonstrated that transcripts involved in HR progression were significantly increased in mESCs as compared with expression in MEFs (Figure 2E; Figures S6 and S7). These data are consistent with our findings of HR protein

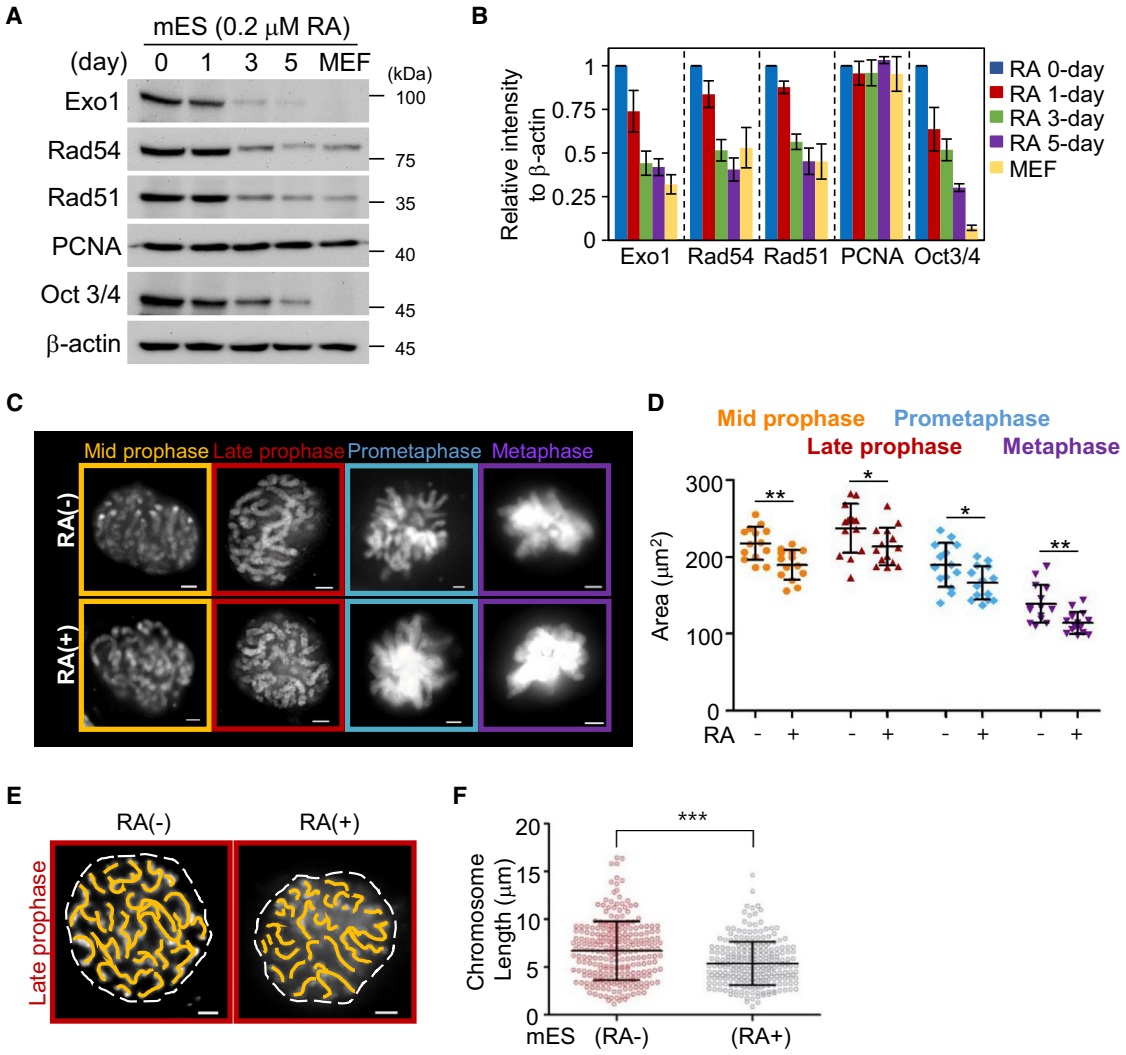

Figure 1. Expression Dynamics of HR Factors and Changes in Global Chromosome Structures

(A) The expression levels of HR factors were determined by immunoblot analysis during cell differentiation. mESCs were spontaneously differentiated by removing leukemia inhibitory factor (LIF) and adding 0.2 μM RA for 5 days. Oct3/4 were used as markers of stemness. (B) The levels of each protein in (A) were quantified, and the ratio relative to β-actin was determined for each time point. The numerical value of each sample was normalized to the numerical value of the sample on day 0. Three independent experiments were performed. Error bars indicate the mean ± SD (n = 3). (C) Chromosome condensation from mid-prophase to metaphase. Fluorescence images of histone H2B-GFP were analyzed in mESCs or differentiated cells (5 days). Scale bars, 2.5 μm. (D) Chromosome volumes of cell nuclei from mid-prophase to metaphase. The nuclei were analyzed with Prism 5 software and the results are reported as the means ± SD (n = 14). Each group was assessed by unpaired Student's t tests (*$p < 0.05$; **$p < 0.01$). (E) Chromosome lengths in late prophase cells were analyzed in mESCs and differentiated cells (5 days). Scale bars, 2.5 μm. (F) Chromosome lengths determined in (E) form histone H2B-GFP nuclei (n = 10). ***$p < 0.001$ (Student's t test).

expression analysis under the same conditions (Figure S1). Moreover, the relative abundance of key HR proteins in ESCs might contribute to survival during extended S-phase or ESC-specific cell-cycle regulation. To further assess S-phase-specific gene expression patterns, we performed Gene Set Enrichment Analysis (GSEA)[29] and found several gene sets significantly upregulated in ESCs, including those involved in DNA recombination, DSB repair, DNA elongation, and DNA repair (Figures 2F and S8), whereas genes regulating cell death and proliferation were downregulated (Figure 2F). This indicates that HR is important throughout the cycle in mESCs, and that high levels of HR factors are mediated by cell-type-specific signaling, but do not result from cell-cycle-specific signaling in mESCs.

Combined Expression of HR Proteins Promotes ESC Differentiation and Prevents the Accumulation of Differentiation-Induced DNA Breaks and Cell Death

HR protein expression decreased during ESC differentiation, which enhanced sensitivity to DNA damage, compared with that in normal

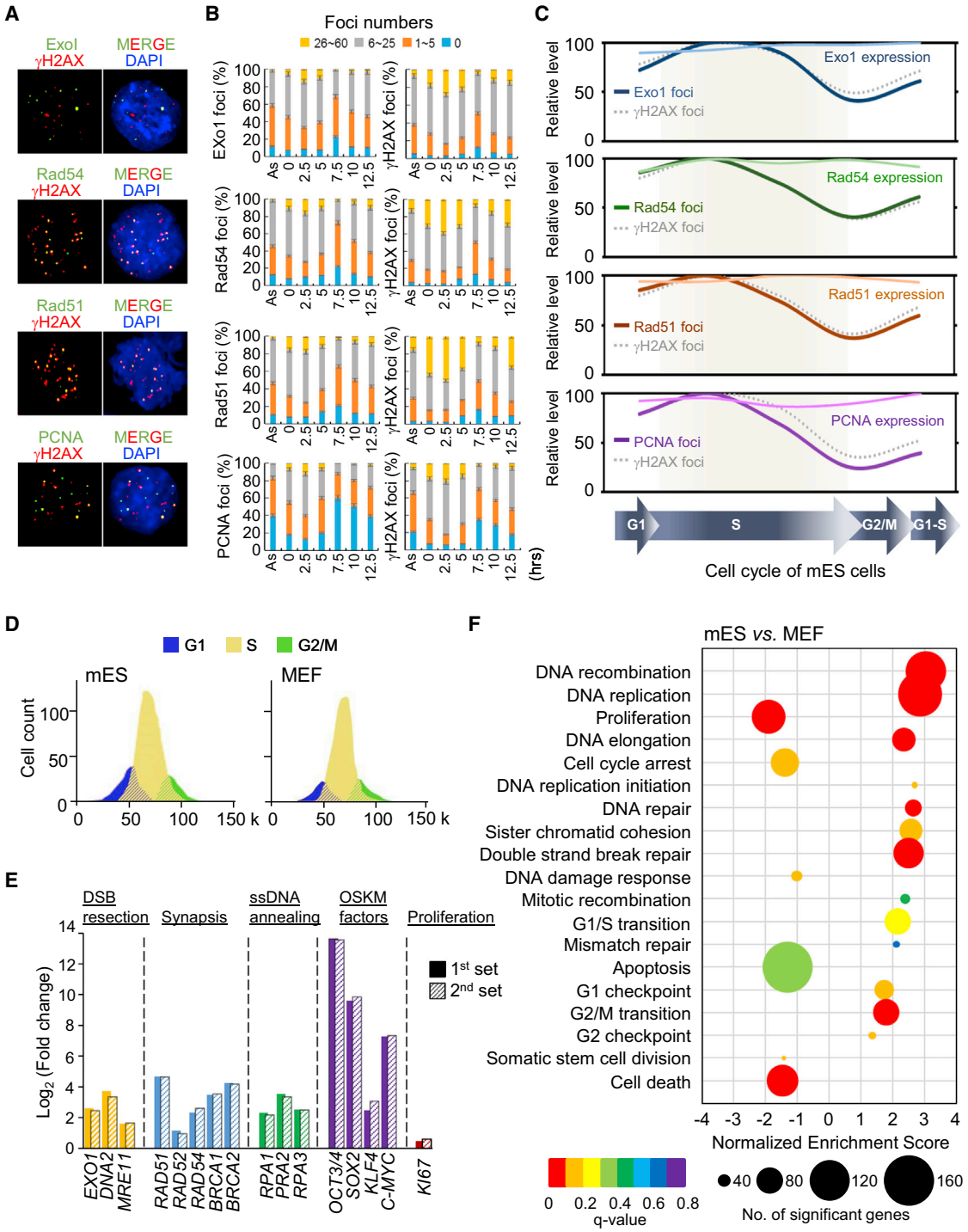

Figure 2. Assembly of Rad51, Rad54, Exo1, and PCNA on Chromatin during S Phase

(A) Representative images of foci formation of HR proteins. mESCs were synchronized by treatment with thymidine and then released from G1/S phase, as shown in Figures S3A and S3B. Cells were immunostained with anti-Rad51, anti-Rad54, anti-Exo1, anti-PCNA, and anti-γH2AX antibodies, and fluorescent signals were categorized as I–IV, according to the number of foci per nucleus (Figure S4). (B) Quantification of foci formation during cell cycle. The number of cells in each category (I–IV) was quantified for each cell-cycle phase (Figures S3 and S4). Error bars indicate the mean ± SD. Three independent time-course experiments were performed, and at least 150 nuclei were counted for each experiment. Error bars indicate the mean ± SD (n = 150–200). (C) The kinetics of protein expression and focus formation with HR factors and PCNA during the cell cycle in mESCs. The cell-cycle phase of mESCs was determined by flow cytometry, and populations of cells in each phase are shown with gradient arrows. The

(legend continued on next page)

mESCs (Figures 1A and S2). These findings are consistent with the low levels of HR protein expression in MEFs (Figure S1). Further, cellular differentiation can induce chromatin reorganization, endogenous DNA breaks, and epigenetic alterations that might affect genome integrity. To investigate whether HR proteins play a functional role in ESC differentiation, we ectopically expressed Rad51, Rad52, and Rad54 in mESCs and analyzed the effect on differentiation and growth (Figures 3 and S9). As expected, mESCs treated with 0.2 μM RA to induce differentiation showed a reduction in the stemness markers Oct3/4 and Nanog (Figures 3B and S10); however, transfected cells with HR factors exhibited a marked reduction in these factors. Remarkably, combined expression of Rad51-Rad52 promotes stem cell differentiation more efficiently compared with that with Rad51 alone (Figures 3A–3D). Thus, the expression of these factors likely enhanced HR activity to facilitate stem cell differentiation via the maintenance of genomic integrity. These results could support the idea that abundant expression of HR proteins throughout the mESC cycle might enhance differentiation efficiency.

ESCs and their differentiated progeny can be identified by cell lineage marker expression analysis. As such, we examined the expression of ectoderm, endoderm, mesoderm, and trophectoderm markers by qPCR analysis in differentiating stem cells with ectopic HR protein expression. Interestingly, ectopic Rad51-Rad52 expression upregulated several lineage markers (with cell proportions of 55% for Nestin, 53% for Gata4, 42.5% for VE-cadherin, and 43.5% for Cdx2 with Rad51-Rad52-Rad54 expression) compared with that in control conditions (17% for Nestin, 36% for Gata4, 23.8% for VE-cadherin, and 33.1% for Cdx2 in the absence of Lif), supporting our previous conclusion that these HR factors enhance HR-mediated DNA repair, and thus promote efficient stem cell differentiation (Figure 3E). Furthermore, the number of surviving cells after differentiation was increased with ectopic Rad51-Rad52 expression (Figure 4A). We also performed comet assays to investigate whether DSBs were similarly reduced in differentiating stem cells with ectopic Rad51-Rad52 expression (Figure 4B). Notably, the induction of HR protein expression resulted in a lower frequency of cells with tail moments, indicating that increased HR proteins can support cell differentiation by repairing chromatin remodeling-induced DNA breaks.

RAD51 Knockdown Induces the Expression of Genes Involved in Checkpoint Activation and Cell Deaths

We performed cell-cycle analyses following *RAD51* knockdown and observed that the G2/M transition was blocked in mESCs, while Rad51 expression in mESCs remained similar to that in MEFs (Figures 1A and 5A–5C). This finding supports the possibility that mESCs require high levels of Rad51 to maintain their cell proliferative capacity even under normal growth conditions (Figures 5B and 5C). We thus directly tested whether *RAD51* knockdown increased the sensitivity to DNA damage in mESCs exposed to 4 mM hydroxyurea (HU) (Figures 5D and S11). In the presence of HU, the rate of cell death increased by 2-fold compared with that in control cells (Figure 5D), suggesting that reduced Rad51 level accelerates cell death following inhibition of the HR-mediated repair pathway.

After showing that *RAD51* knockdown impairs the G2/M transition and induces cell death in mESCs (Figure 5B), we evaluated whether this also affects processes such as apoptosis and cell-cycle progression by performing RNA-seq analysis of the global transcript levels in response to the loss of Rad51 (Figures 5E and S12; Table S2). Gene sets involved in cell-cycle arrest, apoptosis, and cell death were strongly upregulated in response to *RAD51* knockdown (Figure 5E). The level of *GADD45*, which controls stress signals, cell-cycle progression, and apoptosis, increased by 2.54-fold compared with in control cells after treatment with siRAD51, supporting that *RAD51* knockdown causes cell-cycle arrest in the G2/M-phase. As expected, the expression levels of *NAIF1* and *PERP*, which regulate apoptosis, also increased after siRAD51 treatment. In addition, the expression of *KI67*, a proliferation factor, was significantly reduced in response to the loss of Rad51, indicating that HR-deficient stress affects cell-cycle progression (Figure 5E). These results were also associated with increased apoptosis and decreased proliferation, as confirmed in the experiments represented in Figures 5B and 5C. No significant changes in the transcript levels encoding stem cell circuits and numerous components of the HR machinery were observed (Figure 5E). Moreover, qPCR confirmed that changes in gene expression levels were similar to those observed by RNA-seq (Figure 5F; Table S3). Taken together, decreased Rad51 expression impairs cell-cycle progression and leads to apoptosis, indicating that active Rad51-mediated HR is required for self-renewal and cell viability of ESCs.

Absence of Rad51 Increases ssDNA Gaps

We further hypothesized that the loss of Rad51 in mESCs might cause an increase in ssDNA gaps. We assessed localization of the ssDNA-binding protein RPA after siRAD51 treatment in mESCs and analyzed whether those cells undergoing an arrest in G2/M transition would produce additional ssDNA gaps (Figures 5G–5J). In control siRNA transfectants, the average number of RPA foci

time-dependent expression patterns of Exo1, Rad51, Rad54, PCNA, and γH2AX were determined by western blot analysis (Figure S1). The kinetics of cell-cycle-dependent Exo1, Rad51, Rad54, PCNA, and γH2AX focus formation and the disappearance of such foci in the synchronized mESCs were also analyzed. Each measured point represents the mean of 150–200 cells exhibiting more than six foci per cell. The gray dotted lines indicate the percent maximum levels of the γH2AX foci. (D) Flow cytometry analysis of cell-cycle distribution following S-phase synchronization. mESCs and MEFs were synchronized with thymidine and then released from early G1/S-phase. (E) A comparison of gene expression of HR and checkpoint factors after synchronization in S-phase. Bar graph indicates fold change values between mESC and MEFs. Two independent experiments were performed (sets 1 and 2). OSKM, *OCT3/4*, *SOX2*, *KLF4*, and *C-MYC*. (F) GSEA for changes in gene expression of DNA metabolism genes in S-phase of mESCs. GSEA was analyzed with duplicated RNA-seq data from two independent experiments. To adjust for GSEA, we used a false discovery rate (FDR) method by performing calculation based on p values. The q value cutoff to assess statistical significance was set at 0.2, which means that at least 80% of a significant gene set is expected to be true positives.

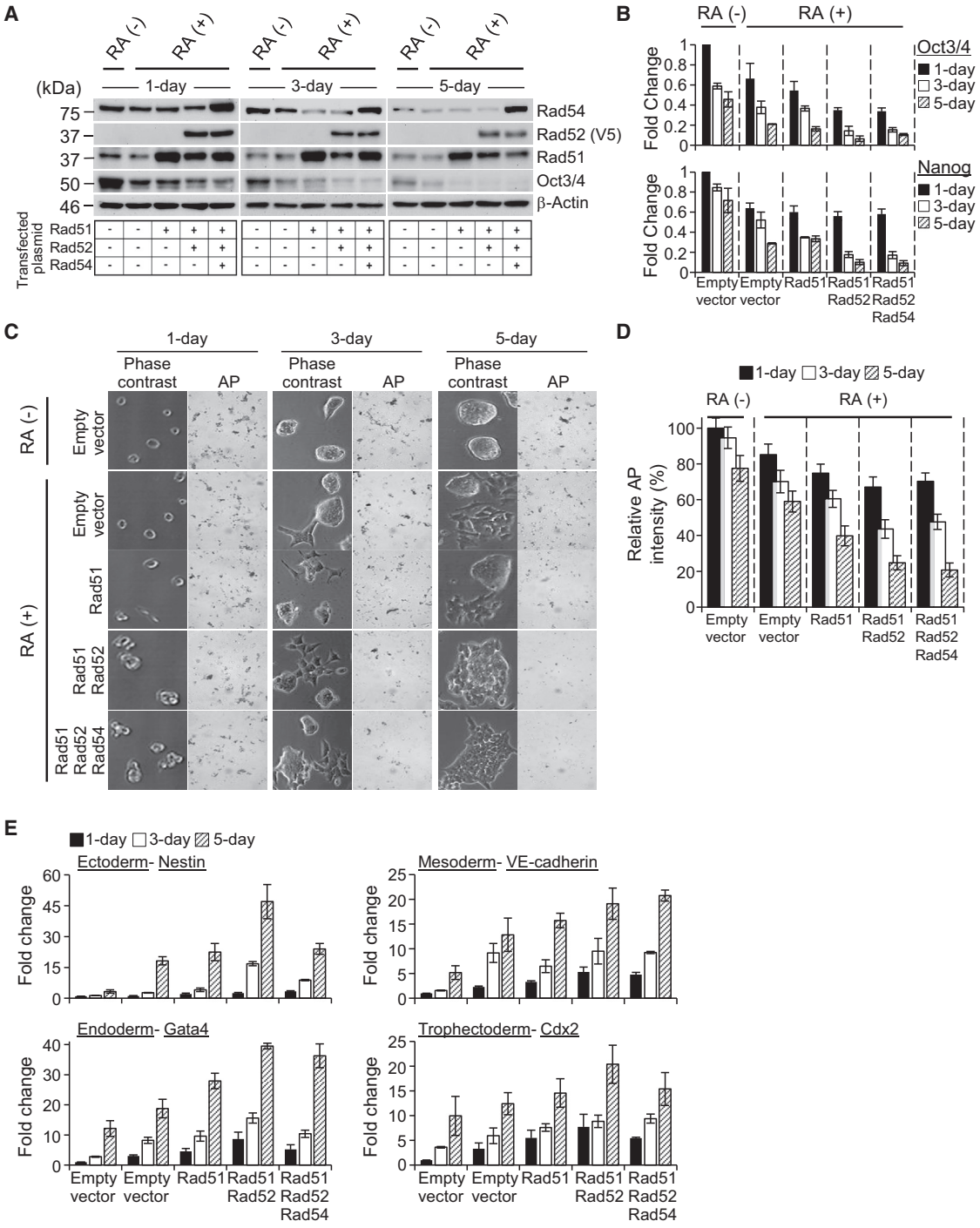

Figure 3. Combined Ectopic Expression of Rad51-Rad52 Promotes Cell Differentiation in mESCs

(A) Expression analysis of HR proteins and Oct3/4. The protein levels of HR factors and Oct3/4 were determined by immunoblot analysis during differentiation. Cell differentiation was induced by removing LIF and adding 0.2 μM RA for 5 days. Rad52 tagging V5 tags at the C terminus were detected using monoclonal V5-tag antibody. Because the cells do not grow indefinitely in *RAD51* depletion (see also Figures 5B and 5C), *RAD51* knockdown experiments could not be performed under these conditions. (B) qPCR analysis of stemness marker genes, Oct3/4 and Nanog, in mESCs after transfection with HR factors. Cells transfected with Rad51 together with Rad52 and Rad54 showed rapid reduction in the expression of stemness markers. Three independent time-course experiments were performed and analyzed by qPCR. Error bars indicate the mean ± SD (n = 3). The fold-change value of each sample was normalized to the numerical value of the sample on 1 day of the RA (–) condition. (C) Phase contrast and

(legend continued on next page)

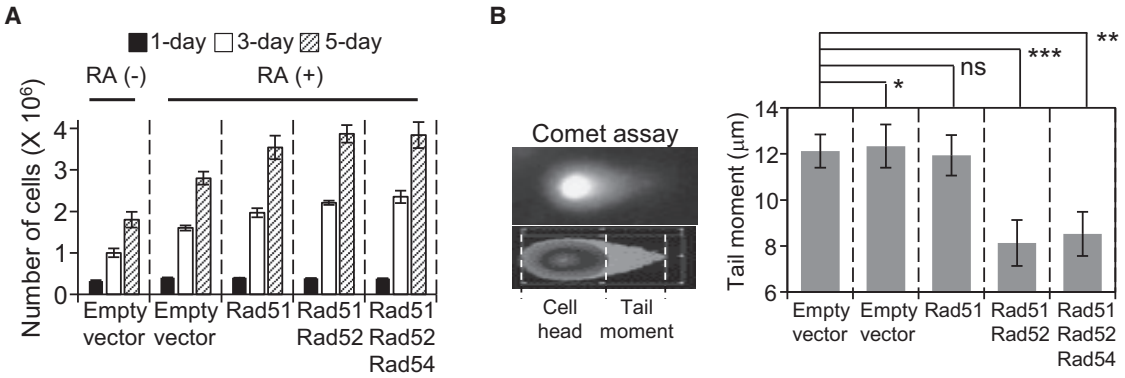

Figure 4. Ectopic Expression of Rad51-Rad52 Exhibits Higher Frequency of Survival for Differentiated Cells

(A) Quantification of cell numbers after mESC differentiation. Three independent experiments were performed and analyzed cell numbers using a hemocytometer. Error bars indicate the mean ± SD (n = 3). (B) Comet assay analyzing DNA damage in individual cells during differentiation. Tail moments of single cells were visualized and measured by Nikon Ti-E fluorescence microcopy. Cell samples were harvested from 3-day-differentiated cell cultures and stained with PI (n = 50). Three independent experiments were performed and analyzed tail moments. Error bars indicate the mean ± SD (n = 3). *$p < 0.05$; **$p < 0.01$; ***$p < 0.001$ (Student's t test). ns, not significant.

was 12.41 ± 5.38. However, this number increased by 1.7-fold after siRAD51 treatment; it was also interesting to note that 44.7% of cells exhibited >20 foci after Rad51 depletion (Figures 5G and 5H). Furthermore, the RPA foci diameter was approximately 280 ± 124 nm in control cells, but increased to 390 ± 171 nm after siRAD51 treatment (Figure 5I). In contrast, MEF cells treated with siRAD51 showed no significant increase in RPA foci diameter (Figure 5I). Thus, HR machinery might affect a post-replication step through the repair of ssDNA gaps, and thereby permit completion of DNA replication to efficiently promote self-renewal and proliferation in ESCs. These results also suggest that Rad51 and its accessory factors such as Rad51AP1, PALB, BRCA1/2, Rad52, and Rad54 could cooperatively prevent additional DNA-break resection that yields larger ssDNA gaps in ESC proliferation or during ESC differentiation.

DISCUSSION

Prolonged inhibition of replication progression generates DNA breaks that stimulate the expression of proteins in the HR-mediated repair pathway.[7,30] Results from a previous study showed that the translation efficiency of Rad51 in mESCs was approximately 6-fold higher than that in MEFs, despite the short half-life of Rad51 in mESCs.[26,31] We hypothesized that the expression of a subset of HR factors that are involved in DSB resection to expose ssDNA ends and in the strand-exchange function of Rad51 might also be elevated in mESCs. We thus presented here that these HR factors are constitutively expressed throughout the cell cycle and respond rapidly to facilitate HR machinery for self-renewal and differentiation by maintaining genomic stability of ESCs. Although a large population of asynchronous ESCs was in the S-phase, this might not be the reason that ESCs exhibited abundance of HR proteins, because synchronized ESCs express these proteins in the entire cell cycle. This observation also correlated with the finding that the expression levels of HR proteins in mESCs following treatment with DNA damage-inducing agents were similar to the corresponding levels in untreated mESCs.[32] Thus, the abundance of HR factors in mESCs might be regulated by specific transcription factors or regulatory signals that mediate global changes in chromosome condensation (Figures 1C–1F). One possible regulatory mechanism involves binding to the *RAD51* and other HR gene promoters by the transcription factor E2F, which is actively involved in cell-cycle progression.[31–34] Furthermore, ESC-specific chromatin dynamics and histone modifications might induce γH2AX phosphorylation, which can contribute to high-level expression of HR factors, their co-localization with γH2AX at ssDNA gaps, and the reversal of forks that are highly prevalent in ESCs (Figures 2A–2C). In support of this idea, the delay in ESC proliferation caused by genomic instability stress was immediately recovered by an HR-dependent repair pathway (Figure 5J). Considering the abundance of HR proteins and their functions in ESC-cycle progression, we propose that Rad51-dependent HR is involved in cellular proliferation, cell-cycle progression, and cell viability, indicating that the HR machinery of ESCs is essential for overcoming genomic instability-related DNA lesions at the replication fork and various types of DNA breaks (Figure 5J). Moreover, our data showed that *RAD51* knockdown in ESCs promotes differential expression of thousands of genes, causing disruption of the cell cycle and leading to cell growth impairment and apoptosis. However, Rad51-Rad52 expression was

alkaline phosphatase-stained images. mESCs transfected with HR factors were stained to measure alkaline phosphatase (AP) activity for each condition of HR gene expression. (D) The relative AP staining intensity during ESC differentiation. Three independent time-course experiments were performed and analyzed for AP intensity using Nikon NIS software. Error bars indicate the mean ± SD (n = 3). (E) qPCR analysis of the expression of diverse lineage markers in spontaneously differentiated mESCs after transfection of HR factors. Three independent time-course experiments were performed and analyzed by qPCR. Error bars indicate the mean ± SD (n = 3). The fold-change value of each sample was normalized to the numerical value of the sample on 1 day of RA (−) condition.

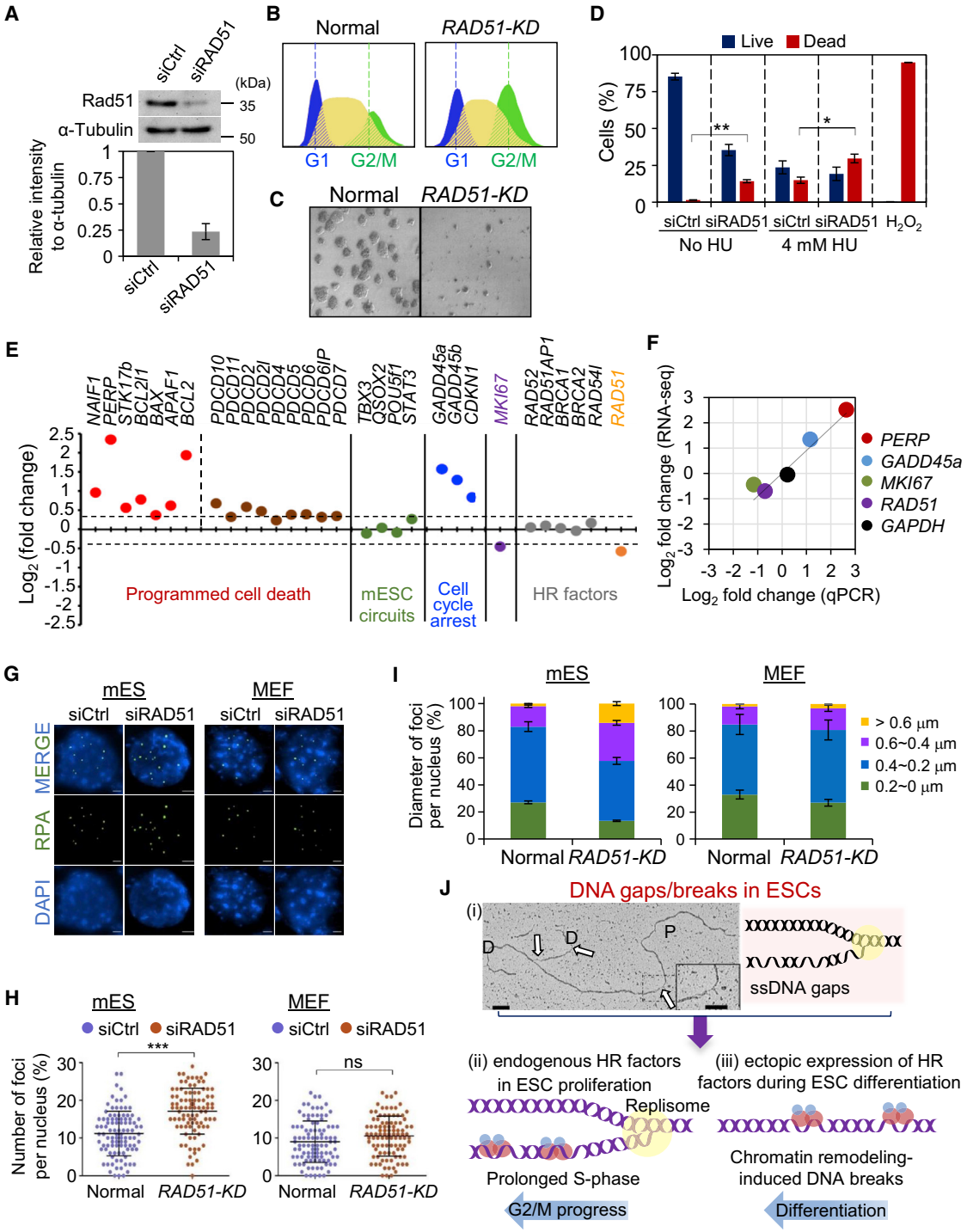

Figure 5. Changes in the Expression Levels of Regulatory Genes in Response to *RAD51* Knockdown

(A) Rad51 protein expression in mESCs was inhibited by transfection with an siRNA pool against Rad51 (siRAD51). Cells transfected with a non-targeting siRNA (siCtrl) were also included. The level of Rad51 relative to α-tubulin was normalized to the mock-transfected sample (bottom). (B) The cell-cycle profiles of mESCs treated with siRAD51 as characterized by FACS analysis. (C) Phase-contrast image of mESCs. (D) Analysis of cell death in mESCs after *RAD51* knockdown. HU (4 mM) was added to mESCs transfected with siCtrl or siRAD51. Cells were stained with thiazole orange/propidium iodide and analyzed by FACS. Three independent experiments were performed and analyzed for cell death. Error bars indicate the mean ± SD (n = 3). *$p < 0.05$; **$p < 0.01$ (Student's t test). (E) Fold-changes in the transcript levels of regulatory genes involved in apoptosis, proliferation, and cell-cycle progression in response to *RAD51* knockdown. The values represent the average fold-changes in expression on a $\log_2$ scale from two

(legend continued on next page)

significantly reduced during ESC differentiation (Figure 1A), which may be caused by cell-specific chromatin remodeling signals and reprogrammed transcriptional regulation. In addition, studies involving systematic analysis of ESCs are required to identify the factors that directly regulate HR gene expression and determine the nature of HR protein modifications during self-renewal and differentiation.

Stem cells can undergo self-renewal and differentiation into diverse lineages. During stem cell differentiation, chromatin structural changes are observed in conjunction with regulatory changes of transcription factors,[35,36] which can alter DNA damage sensitivity. Further, reduced HR protein expression may be a general feature of stem cell differentiation, which could result in cellular progression defects and DNA damage accumulation. DNA damage to the genome, if not repaired properly, will cause premature aging, arrest of cell proliferation, aneuploidy, and apoptosis of stem cells. We analyzed diverse biological phenomena associated with differentiation after combined ectopic expression of Rad51-Rad52 and observed that ESCs expressing HR proteins exhibit the following: (1) rapid and efficient cell differentiation, (2) higher frequency of differentiation-lineage markers, (3) reduction of chromosome fragmentation, and (4) higher frequency of survival for differentiated cells. Consistent with these observations, large numbers of ESCs are effectively differentiated into multiple lineages. Thus, a combination of Rad51-Rad52 is likely sufficient to promote cell differentiation via HR-mediated repair of DNA breaks caused by chromatin remodeling (Figure 5J). As we suggested previously, HR proteins orchestrate DNA break repair and G2/M progression during self-renewal of ESCs. These abundant HR proteins might immediately support DNA repair caused by dynamic changes to chromatin during ESC differentiation.

Here, we provided evidence that mESCs control the expression and activation of multiple genes involved in diverse functions associated with DNA metabolism, including DNA repair and homologous recombination, through specific mechanisms that differ from those utilized in differentiated cells. Because differentiating stem cells downregulate HR-mediated DNA repair proteins, the development of techniques for promoting timely cellular progression and to maintain genomic integrity against DNA damage during differentiation are required. Importantly, our strategy for combinatorial expression of HR proteins during cellular differentiation could provide high-quality ESCs, for therapies to treat human disease, as a source of diverse differentiated cell types.

MATERIALS AND METHODS

Cell Culture

The J1 mESC line and MEFs used in this study were described previously.[26] J1 cells were cultured in DMEM plus GlutaMAX-I (10569; GIBCO), which was supplemented with 10% (v/v) horse serum (16050-122; GIBCO), 10 mM HEPES (15630-080; GIBCO), 2 mM L-glutamine (25030-081; GIBCO), 0.1 mM Minimum Essential Medium Non-Essential Amino Acids (11140-050; GIBCO), 0.1 mM β-mercaptoethanol (21985-023; GIBCO), 100 U/mL penicillin-100 μg/ml streptomycin (15140-122; GIBCO), and 1,000 U/mL mouse ESGRO leukemia inhibitory factor (LIF) (ESG 1107; Millipore) at 37°C in a humidified environment with 5% CO_2. J1 cells were plated on cell-free feeder plates coated with 0.1% gelatin for each experiment. MEFs were cultured in DMEM plus 10% (v/v) fetal bovine serum (16000-044; GIBCO) and 100 U/mL penicillin-100 μg/ml streptomycin (15140-122; GIBCO) at 37°C in a humidified environment with 5% CO_2. H9 hESCs were a gift from Dr. Park (CHA University, South Korea), and the cells were cultured in DMEM/F-12 (11320-033; GIBCO) supplemented with 1% (v/v) non-essential amino acid (NEAA), 1% β-mercaptoethanol (21985-023; GIBCO), 100 U/mL penicillin-100 μg/mL streptomycin (15140-122; GIBCO), 20% KnockOut Serum Replacement (10828-028; GIBCO), and 4 ng/mL basic fibroblast growth factor (bFGF) Recombinant Human Protein (13256-029; GIBCO) on mitomycin C-treated MEFs, with the media replaced every day.

Western Blot Analysis

Samples were prepared as described previously.[26] The antibodies against Rad51 (sc-8349, 1:2,000), Rad54 (sc-374598, 1:2,000), and PCNA (sc-56, 1:2,000) were purchased from Santa Cruz Biotechnology. The antibody against Exo1 (MS-1534, 1:1,000) was purchased from Thermo Scientific. The antibodies against β-actin (ab8226, 1:10,000) and α-tubulin (sc-8035, 1:10,000), which were used as loading controls, were purchased from Abcam and Santa Cruz Biotechnology, respectively.

Induction of Differentiation

The differentiation of mESCs was induced by removing LIF from the culture medium and adding 0.2 μM all-*trans*-RA (R2625; Sigma) for

independent RNA-seq experiments. The values of the dotted lines (±0.32 $\log_2$) represent the fold-change in α-actin expression from four independent RNA-seq experiments. (F) Changes in gene expression analyzed by RNA-seq compared with qPCR results. Log_2 values of fold-changes measured in terms of the fragments-per-kilobase of exon per million fragments (FPKM) compared with fold-changes in mRNA expression detected by qPCR analysis. (G) Representative images of RPA foci formation in mESCs and MEFs under each indicated condition. Scale bars, 2.5 μm. (H) Analysis of RPA foci formation after *RAD51* knockdown. mESCs or MEFs transfected with siCtrl and the siRAD51 pool at 48 hr post-transfection. The scatterplots show the number of RPA foci per single cell (mean ± SD, n = 83 nuclei). Error bars indicate the mean ± SD. ***$p < 0.001$ (Student's t test). (I) Accumulation of larger ssDNA gaps in the *RAD51* knockdown condition. The diameters of RPA foci were quantified in normal cells and siRAD51-treated cells. At least 80 nuclei were counted for each experiment. Error bars indicate the mean ± SD. (J) Roles of HR factors in self-renewal and differentiation of ESCs. (i) Electron micrograph of a replication fork in mESCs.[5] White arrows indicate ssDNA gaps. Scale bar, 500 bp (200 bp in inset). (ii) HR proteins are constitutively expressed throughout the cell cycle in ESCs. Therefore, the HR-mediated DNA repair can operate rapidly to repair ssDNA gaps and DNA damage, and to overcome replication-associated stresses. (iii) During differentiation, ectopic expression of HR proteins allows for the repair of differentiation-induced DNA breaks or abnormal signaling-related genomic instability, which induces an arrest in cellular progression. D, daughter duplex DNA; ns, not significant; P, parental duplex DNA.

5 days. To prepare expression vector of HR genes, we subcloned amplified cDNAs of *RAD51*, *RAD52*, and *RAD54* genes into pcDNA3.1(+) vector (*Hind*III/*BamH*I sites for *RAD51*; *EcoR*I/*Not*I sites for *RAD52*; *Hind*III/*BamH*I sites for *RAD54*). For transfection of HR gene expression vectors, total 2 μg plasmid DNA carrying each gene was mixed with polyethylenimine (PEI) and added to the identical cultures. The culture medium was changed after 48 hr, and differentiation was induced as described above.

Cell Death Analysis

Cells were harvested and washed with PBS briefly. To analyze cell death, we added 2 μL of thiazole orange (TO; 349483; BD) solution and 1 μL of propidium iodide (PI) (349483; BD) solution to the cell suspension. The final staining concentrations were 84 nM for TO and 4.3 μM for PI. The samples were incubated at 25°C, then analyzed using a FACSCalibur flow cytometer (Becton Dickinson) and quantified with FlowJo software (Tree Star).

Immunofluorescence Analysis

Cells were grown on poly-L-lysine-coated coverslips and then treated with 1% paraformaldehyde. The cells were then permeabilized with 0.1% Triton X-100. The cells were blocked with 3% BSA in PBS with 0.1% Tween 20 (T-PBS) and then incubated with the following primary antibodies, diluted at the indicated ratios: anti-RPA (#2208, 1:200; Cell Signaling), anti-Rad51 (sc-8349, 1:200; Santa Cruz), anti-Rad54 (sc-374598, 1:200; Santa Cruz), and anti-Exo1 (MS-1534-P, 1:100; Thermo). After washing three times with T-PBS, cells were incubated for 1 hr with appropriate anti-Alexa 488 (111-545-003, 1:500; Jackson), anti-fluorescein isothiocyanate (FITC) (112-095-003, 1:500; Jackson), anti-Cy3 (111-165-003, 1:500; Jackson)-conjugated secondary antibodies and then mounted using a mounting solution containing DAPI. Images were captured using an Eclipse Ti-E fluorescence microscope (Nikon, Tokyo, Japan) equipped with fluorescence filters for DAPI and the indicated fluorophores conjugated to the secondary antibodies.

Chromosome Analysis

mESCs expressing H2B-GFP were attached on 12-mm coverglass coated by poly-L-lysine and then were fixed with 1% paraformaldehyde for 5 min. For nuclei staining, cells were stained with mounting solution containing 2 μg/ml DAPI. H2B-GFP cells were observed on an inverted Eclipse Ti-E fluorescence microscope. A complete z stack with a step size of 0.25 μm (20 images per stack) was acquired using Nikon NIS software. Chromosome volume and length were analyzed using Nikon NIS software.

Antibodies

The following primary antibodies were used: anti-rabbit Rad51 (sc-8349, 1:2,000; Santa Cruz), anti-mouse Rad54 (sc-374598 1:2,000; Santa Cruz), anti-mouse PCNA (sc-56, 1:2,000; Santa Cruz), anti-mouse Exo1 (MS-1534, 1:1,000; Thermo Fisher), anti-mouse Oct3/4 (sc-5297, 1:3,000; Santa Cruz), anti-rat RPA (#2208, 1:200; Cell Signaling), anti-mouse β-Actin (ab8226, 1:10,000; Abcam), and anti-mouse α-tubulin (sc-8035, 1:10,000; Santa Cruz). The following secondary antibodies were used: anti-mouse Alexa 488 (111-545-003, 1:500; Jackson), anti-rat fluorescein isothiocyanate (FITC) (112-095-003, 1:500; Jackson), and anti-rabbit Cy3 (111-165-003, 1:500; Jackson).

RNAi

To knock down the expression of Rad51, we added siGENOME siRNA SMARTpool (M-062730-01-005; Dharmacon) against the Rad51 gene in mESCs. This siRNA pool was composed of a mixture of four different targeting oligonucleotides with the following sequences: 5′-CAUCAUCGCUCAUGCGUCA-3′, 5′-UGUCAUACGUUGGCUGUUA-3′, 5′-GGUAAUCACCAACCAGGUA-3′, and 5′-GAGAUCAUACAGAUAACUA-3′. DharmaFECT-1 (T-2001; Dharmacon) was used to perform siRNA transfection according to the manufacturer's instructions. A non-targeting siRNA (siCtrl) was used as a negative control (ON-TARGETplus non-targeting pool; Dharmacon). The cells were harvested and analyzed 48 hr post-transfection.

Comet Assay

mESCs were resuspended in 1× PBS and added to 400 μL of molten (40°C) 1% low-melting temperature agarose (LMA) (50101; Takara) gel to achieve the cell density to 3×10^4 cells/mL. The LMA was pipetted onto the microscope slides. Slides were stored to allow agarose to gel for about 2 min. Slides were immersed in the lysis buffer (2% sodium lauroyl sarcosinate, 0.5 M Na2EDTA, 0.5 mg/mL Proteinase K [pH 8.0]) for 20 hr at 37°C. Slides were removed from lysis buffer and submerged in room temperature rinse buffer for 30 min at room temperature. Electrophoresis was conducted at 20 V, 7 mA, for 20 min. The slides were then washed in a rinse buffer (90 mM Tris, 90 mM boric acid, 2 mM Na2EDTA [pH 8.5]) for 5 min for three times. The slides were stained with staining solution containing 2.5 μg/mL propidium iodide in 1× PBS for 20 min and observed with a fluorescent microscope. Quantification of DNA tail was performed using CASP software of 1.2.3beta2 version.

RNA Isolation

Total RNA was isolated using the TRIzol reagent (Invitrogen). RNA quality was assessed with an Agilent 2100 Bioanalyzer (Agilent Technologies), and RNA concentration was quantified using an ND-2000 Spectrophotometer (Thermo).

qPCR

1 μg of total RNA was reverse transcribed using SuperiorScript II Reverse transcriptase (Enzynomics). qPCR was performed with a SYBR Green PCR kit (Invitrogen) and the Applied Biosystems Real-Time PCR system. Oligo sequences are listed in Table S3.

mRNA-Seq Library Preparation and Sequencing

For each RNA sample, library construction was performed using the SENSE mRNA-Seq Library Prep Kit (Lexogen) according to the manufacturer's instructions. In brief, 2 μg of total RNA was prepared from each sample and incubated with magnetic beads coated with oligo-dT, after which all RNAs (except for mRNAs) were removed with a

washing solution provided in the kit. Library was produced by the random hybridization of heterodimers (starter/stopper) to the poly(A) RNA bound to the magnetic beads. These heterodimers contained Illumina-compatible linker sequences. Reverse transcription and ligation reaction was performed to extend the starter to the next hybridized heterodimer. High-throughput sequencing was performed as paired-end 100 sequencing using a HiSeq 2000 instrument (Illumina, USA).

Gene Set Enrichment Analysis

To investigate whether the two cell types (e.g., mESC versus MEF) were significantly different, GSEA, a bioinformatics method, was performed using a program provided by the Broad Institute (https://software.broadinstitute.org/gsea/index.jsp). Differences in gene expression levels between two cell types were considered significant if most of the gene members were in the upregulated (top-ranked) or downregulated (bottom ranked) region of the profile. Based on the Kolmogorov-Smirnov test (K-S test), the GSEA calculated an enrichment score for the two cell types to measure the degree to which the gene expression level for each of the cell types was enriched in the upregulated or downregulated region of the profile. A normalized enrichment score was calculated from the enrichment score to determine the number of significant genes.

Data Analysis

mRNA-seq reads were mapped using the TopHat software tool in order to obtain an alignment file. We used the University of California Santa Cruz (UCSC) mm10 sequence as a reference sequence. We used the fragments-per-kilobase of exon per million fragments (FPKM) method to determine the expression levels of gene regions. A global normalization method was used for comparisons between samples. Gene classification was based on searches in the DAVID (https://david.ncifcrf.gov/) and Medline databases (https://www.ncbi.nlm.nih.gov/).

Statistical Analysis

Data were analyzed through Prism 5 software and reported as the means ± SEM or ± SD. Statistically significant differences from multiple groups were assessed by unpaired Student's t tests. Statistical significances were set at $^{*}p < 0.05$, $^{**}p < 0.01$, and $^{***}p < 0.001$. All experiments were performed and analyzed in triplicate.

Accession Numbers

RNA-seq reads are available under the following accession numbers in the NCBI Sequence Read Archive: SRX2030573, SRX2030574, and SRX2030575.

SUPPLEMENTAL INFORMATION

Supplemental Information includes twelve figures and three tables and can be found with this article online at https://doi.org/10.1016/j.ymthe.2018.02.003.

AUTHOR CONTRIBUTIONS

E.-H.C. and K.P.K. designed and structured the experiments. E.-H.C. and S.Y. performed the experiments. E.-H.C. and K.P.K. analyzed data and wrote the manuscript. All authors gave final approval of the manuscript.

CONFLICTS OF INTEREST

The authors declare no conflict of interest.

ACKNOWLEDGMENTS

This work was supported by grants to K.P.K. from the National Research Foundation of Korea funded by the Ministry of Science, ICT & Future Planning (2017R1A2B2005603) and the Next-Generation BioGreen 21 Program (SSAC; PJ01322801), Rural Development Administration, Republic of Korea.

REFERENCES

1. Keller, G.M. (1995). In vitro differentiation of embryonic stem cells. Curr. Opin. Cell Biol. *7*, 862–869.
2. Smith, A.G. (2001). Embryo-derived stem cells: of mice and men. Annu. Rev. Cell Dev. Biol. *17*, 435–462.
3. Tichy, E.D., and Stambrook, P.J. (2008). DNA repair in murine embryonic stem cells and differentiated cells. Exp. Cell Res. *314*, 1929–1936.
4. Giachino, C., Orlando, L., and Turinetto, V. (2013). Maintenance of genomic stability in mouse embryonic stem cells: relevance in aging and disease. Int. J. Mol. Sci. *14*, 2617–2636.
5. Ahuja, A.K., Jodkowska, K., Teloni, F., Bizard, A.H., Zellweger, R., Herrador, R., Ortega, S., Hickson, I.D., Altmeyer, M., Mendez, J., and Lopes, M. (2016). A short G1 phase imposes constitutive replication stress and fork remodelling in mouse embryonic stem cells. Nat. Commun. *7*, 10660.
6. Maynard, S., Swistowska, A.M., Lee, J.W., Liu, Y., Liu, S.T., Da Cruz, A.B., Rao, M., de Souza-Pinto, N.C., Zeng, X., and Bohr, V.A. (2008). Human embryonic stem cells have enhanced repair of multiple forms of DNA damage. Stem Cells *26*, 2266–2274.
7. Krejci, L., Altmannova, V., Spirek, M., and Zhao, X. (2012). Homologous recombination and its regulation. Nucleic Acids Res. *40*, 5795–5818.
8. McGill, C.B., Shafer, B.K., Derr, L.K., and Strathern, J.N. (1993). Recombination initiated by double-strand breaks. Curr. Genet. *23*, 305–314.
9. Puchta, H., Dujon, B., and Hohn, B. (1993). Homologous recombination in plant cells is enhanced by in vivo induction of double strand breaks into DNA by a site-specific endonuclease. Nucleic Acids Res. *21*, 5034–5040.
10. Rouet, P., Smih, F., and Jasin, M. (1994). Introduction of double-strand breaks into the genome of mouse cells by expression of a rare-cutting endonuclease. Mol. Cell. Biol. *14*, 8096–8106.
11. Zhang, N., Liu, X., Li, L., and Legerski, R. (2007). Double-strand breaks induce homologous recombinational repair of interstrand cross-links via cooperation of MSH2, ERCC1-XPF, REV3, and the Fanconi anemia pathway. DNA Repair (Amst.) *6*, 1670–1678.
12. Rothstein, R., Michel, B., and Gangloff, S. (2000). Replication fork pausing and recombination or "gimme a break". Genes Dev. *14*, 1–10.
13. Hong, S., Sung, Y., Yu, M., Lee, M., Kleckner, N., and Kim, K.P. (2013). The logic and mechanism of homologous recombination partner choice. Mol. Cell *51*, 440–453.
14. Hunter, N. (2015). Meiotic recombination: the essence of heredity. Cold Spring Harb. Perspect. Biol. *7*, a016618.
15. Cerbinskaite, A., Mukhopadhyay, A., Plummer, E.R., Curtin, N.J., and Edmondson, R.J. (2012). Defective homologous recombination in human cancers. Cancer Treat. Rev. *38*, 89–100.
16. Helleday, T. (2010). Homologous recombination in cancer development, treatment and development of drug resistance. Carcinogenesis *31*, 955–960.
17. Jasin, M., and Rothstein, R. (2013). Repair of strand breaks by homologous recombination. Cold Spring Harb. Perspect. Biol. *5*, a012740.

18. Lambert, S., and Lopez, B.S. (2000). Characterization of mammalian RAD51 double strand break repair using non-lethal dominant-negative forms. EMBO J. *19*, 3090–3099.

19. Lord, C.J., and Ashworth, A. (2012). The DNA damage response and cancer therapy. Nature *481*, 287–294.

20. Lok, B.H., Carley, A.C., Tchang, B., and Powell, S.N. (2013). RAD52 inactivation is synthetically lethal with deficiencies in BRCA1 and PALB2 in addition to BRCA2 through RAD51-mediated homologous recombination. Oncogene *32*, 3552–3558.

21. van Veelen, L.R., Essers, J., van de Rakt, M.W., Odijk, H., Pastink, A., Zdzienicka, M.Z., Paulusma, C.C., and Kanaar, R. (2005). Ionizing radiation-induced foci formation of mammalian Rad51 and Rad54 depends on the Rad51 paralogs, but not on Rad52. Mutat. Res. *574*, 34–49.

22. Dixon, J.R., Jung, I., Selvaraj, S., Shen, Y., Antosiewicz-Bourget, J.E., Lee, A.Y., Ye, Z., Kim, A., Rajagopal, N., Xie, W., et al. (2015). Chromatin architecture reorganization during stem cell differentiation. Nature *518*, 331–336.

23. Zwaka, T.P., and Thomson, J.A. (2003). Homologous recombination in human embryonic stem cells. Nat. Biotechnol. *21*, 319–321.

24. Sengupta, S., Robles, A.I., Linke, S.P., Sinogeeva, N.I., Zhang, R., Pedeux, R., Ward, I.M., Celeste, A., Nussenzweig, A., Chen, J., et al. (2004). Functional interaction between BLM helicase and 53BP1 in a Chk1-mediated pathway during S-phase arrest. J. Cell Biol. *166*, 801–813.

25. Mandal, P.K., Blanpain, C., and Rossi, D.J. (2011). DNA damage response in adult stem cells: pathways and consequences. Nat. Rev. Mol. Cell Biol. *12*, 198–202.

26. Yoon, S.W., Kim, D.K., Kim, K.P., and Park, K.S. (2014). Rad51 regulates cell cycle progression by preserving G2/M transition in mouse embryonic stem cells. Stem Cells Dev. *23*, 2700–2711.

27. Bártová, E., Krejcí, J., Harnicarová, A., Galiová, G., and Kozubek, S. (2008). Histone modifications and nuclear architecture: a review. J. Histochem. Cytochem. *56*, 711–721.

28. Meshorer, E. (2008). Imaging chromatin in embryonic stem cells. In StemBook (Harvard Stem Cell Institute), 10.3824/stembook.1.2.1, https://www.ncbi.nlm.nih.gov/books/NBK27072/.

29. Trapnell, C., Roberts, A., Goff, L., Pertea, G., Kim, D., Kelley, D.R., Pimentel, H., Salzberg, S.L., Rinn, J.L., and Pachter, L. (2012). Differential gene and transcript expression analysis of RNA-seq experiments with TopHat and Cufflinks. Nat. Protoc. *7*, 562–578.

30. Saintigny, Y., Delacôte, F., Varès, G., Petitot, F., Lambert, S., Averbeck, D., and Lopez, B.S. (2001). Characterization of homologous recombination induced by replication inhibition in mammalian cells. EMBO J. *20*, 3861–3870.

31. Tichy, E.D., Pillai, R., Deng, L., Tischfield, J.A., Hexley, P., Babcock, G.F., and Stambrook, P.J. (2012). The abundance of Rad51 protein in mouse embryonic stem cells is regulated at multiple levels. Stem Cell Res. (Amst.) *9*, 124–134.

32. Choi, E.H., Yoon, S., Park, K.S., and Kim, K.P. (2017). The homologous recombination machinery orchestrates post-replication DNA repair during self-renewal of mouse embryonic stem cells. Sci. Rep. *7*, 11610.

33. Dyson, N. (1998). The regulation of E2F by pRB-family proteins. Genes Dev. *12*, 2245–2262.

34. Bracken, A.P., Ciro, M., Cocito, A., and Helin, K. (2004). E2F target genes: unraveling the biology. Trends Biochem. Sci. *29*, 409–417.

35. Nashun, B., Hill, P.W., and Hajkova, P. (2015). Reprogramming of cell fate: epigenetic memory and the erasure of memories past. EMBO J. *34*, 1296–1308.

36. Tran, H., Almeida, S., Moore, J., Gendron, T.F., Chalasani, U., Lu, Y., Du, X., Nickerson, J.A., Petrucelli, L., Weng, Z., and Gao, F.B. (2015). Differential toxicity of nuclear RNA foci versus dipeptide repeat proteins in a Drosophila model of C9ORF72 FTD/ALS. Neuron *87*, 1207–1214.